AGU ADVANCING EARTH AND SPACE SCIENCE

Geophysical Research Letters®

RESEARCH LETTER
10.1029/2021GL095525

Key Points:

- Negative return strokes with peak currents larger than 150 kA in winter in Japan produce unusual electric field change waveforms
- These strongest negative return strokes are preceded by a fast downward negative leader with short duration and large peak current
- The preceding downward negative leader may be associated with downward terrestrial gamma-ray flashes

Supporting Information:

Supporting Information may be found in the online version of this article.

Correspondence to:

T. Wu,
tingwu@gifu-u.ac.jp

Citation:

Wu, T., Wang, D., Huang, H., & Takagi, N. (2021). The strongest negative lightning strokes in winter thunderstorms in Japan. *Geophysical Research Letters*, *48*, e2021GL095525. https://doi.org/10.1029/2021GL095525

Received 31 JUL 2021
Accepted 19 OCT 2021

The Strongest Negative Lightning Strokes in Winter Thunderstorms in Japan

Ting Wu[1], Daohong Wang[1], Haitao Huang[1], and Nobuyuki Takagi[1]

[1]Department of Electrical, Electronic, and Computer Engineering, Gifu University, Gifu, Japan

Abstract Winter thunderstorms in Japan are well known for the frequent production of energetic positive cloud-to-ground (CG) lightning flashes. By contrast, strong negative CG flashes or negative return strokes in winter thunderstorms are largely unknown. In this study, we demonstrate that negative return strokes with peak currents larger than 150 kA (absolute value) in winter thunderstorms in Japan mostly produce electric field change waveforms that are different from those of normal return strokes. Due to their unusual waveforms, these strongest negative strokes have not been recognized as return strokes by the lightning research community. We further demonstrate that these strong negative return strokes are preceded by a fast downward negative leader with a short duration and strong peak current. We suggest that the fast and powerful downward negative leader may be associated with downward terrestrial gamma-ray flashes. We also present evidence that these strong negative strokes are likely "superbolts" observed from space.

Plain Language Summary The negative return stroke is the most well studied lightning discharge process. In this study, we demonstrate that negative return strokes with peak currents larger than 150 kA in winter thunderstorms in Japan mostly produce unique electric field change waveforms that are generally different from those of normal return strokes. Due to their unusual waveforms, these strongest negative strokes have not been recognized as return strokes by the lightning research community and may not be correctly identified by nationwide lightning location systems.

1. Introduction

Lightning discharges in winter thunderstorms in Japan exhibit many unique features. The most well known feature is the frequent production of positive cloud-to-ground (CG) lightning flashes (Brook et al., 1982; Takeuti et al., 1978). Exceptionally powerful and energetic positive CG flashes in winter thunderstorms have been observed and investigated extensively and are known to induce transient luminous events such as sprites and elves (Adachi, 2005; Hayakawa, 2004; Matsudo et al., 2007; Suzuki et al., 2006; Wang et al., 2021). By contrast, strong negative CG flashes or return strokes in winter thunderstorms are much less well known.

Strong electric field change (E-change) pulses with the same polarity as those of negative return strokes in winter thunderstorms in Japan have been reported by a few studies but their physical mechanism is not yet clear. Ishii and Saito (2009) reported strong electric field change (E-change) waveforms that were associated with transmission-line faults in winter along the Japan Sea coast. Some of the waveforms had the same polarity as those produced by negative return strokes but were quite different from those of typical return strokes. Ishii and Saito (2009) attributed these waveforms to upward lightning. Wu et al. (2014) reported the so-called "large bipolar events" (LBEs) that produced characteristic large and bipolar E-change waveforms. LBEs were almost always found on land so they were believed to be associated with tall objects. Wada et al. (2020) observed two downward terrestrial gamma-ray flashes (TGFs) in winter thunderstorms and found that both TGFs were associated with strong pulses with estimated peak currents of −260 kA and −197 kA. These strong pulses were quite similar to those reported by Ishii and Saito (2009) and were interpreted by Wada et al. (2020) as energetic in-cloud pulses (Lyu et al., 2015), which is a type of intracloud discharge closely associated with TGFs. Similar strong pulses were also reported by Wu et al. (2020b) to trigger upward negative leaders from tall objects. Wu et al. (2020b) speculated that these strong pulses were produced by special negative return strokes. These scarce and contradictory reports of strong negative discharges fully reveal how little we know about negative strokes in winter thunderstorms.

In this study, we will demonstrate that negative return strokes with estimated peak currents larger than 150 kA (absolute value) in winter thunderstorms in Japan mostly produce E-change waveforms that are generally different from normal return stroke waveforms but are very similar to strong pulses reported by the above-mentioned studies. Our results also indicate that many, if not all, of the strong pulses reported by previous studies, were also produced by strong negative return strokes. Due to the unusual waveforms, the existence of these strongest negative return strokes is not yet recognized by the lightning research community, and at least some of these strokes are apparently not identified by nationwide lightning location systems.

2. Observation and Data

2.1. Winter Observation With the FALMA

A fast antenna lightning mapping array (FALMA) system including 14 observation sites were set up for the winter observation in the Hokuriku region of Japan from December 2018 to March 2019. Locations of these 14 sites are shown in Figure S1 in Supporting Information S1 and can also be found in our previous studies (e.g., Wu et al., 2020b). The FALMA is a low-frequency lightning mapping system using fast antennas as the sensors (Wu et al., 2018). Every site records E-change waveforms in the frequency range of 500 Hz to 500 kHz with a sampling rate of 10 MHz. The FALMA is capable of high-quality 3-D lightning mapping. However, during the winter observation, due to the fact that winter lightning discharges are close to the ground and are usually very complicated, location results of source height are not reliable (Wu et al., 2020a), so we will only use 2-D location results in this study.

The atmospheric electricity sign convention is used in this study, so a negative return stroke produces a positive E-change waveform.

2.2. Data Selection

In this study, we will analyze negative strokes with estimated peak currents larger than 150 kA (absolute value). Peak currents are estimated by correlating normalized E-change magnitudes with peak currents reported by the Japanese Lightning Detection Network (JLDN; Matsui et al., 2019) as described by Wu et al. (2021). We identified all pulses having the same polarity as negative return strokes and having estimated peak currents larger than 150 kA in a 150×150 km^2 area shown in Figure S1 in Supporting Information S1. A total of 104 pulses were identified. We will demonstrate that these strong pulses are produced by negative return strokes. Locations of these strokes are also shown in Figure S1 in Supporting Information S1.

Among the identified 104 strokes, 6 strokes saturated all FALMA sites. These six strokes are not included in the analyses of this study but their E-change waveforms are shown in Figure S2 in Supporting Information S1. E-change waveform figures of the remaining 98 strokes are provided in the data repository.

2.3. LAPOS Observation of a Strong Stroke

A stroke with a JLDN-reported peak current of −335 kA was observed in December of 2020 by the FALMA as well as a high-speed optical system called Lightning Attachment Process Observation System (LAPOS; Wang et al., 2013) and is analyzed separately in Section 3.3. The LAPOS was set up at the same location as the FALMA site represented by a red square in Figure S1 in Supporting Information S1. A detailed description of the LAPOS used for this study can be found in Wang et al. (2013). The LAPOS contains 14 photodiodes including 7 photodiodes with high sensitivity and 7 with low sensitivity. Photodiodes with high and low sensitivities are aligned alternatively in the vertical direction, and each photodiode is configured to measure the light intensity at a certain elevation angle. Light intensity waveforms from 14 photodiodes along with the GPS signal are recorded by an oscilloscope with a sampling rate of 10 MHz. Details of the location and the field of view of the LAPOS with respect to the stroke can be found in Figure S3 in Supporting Information S1.

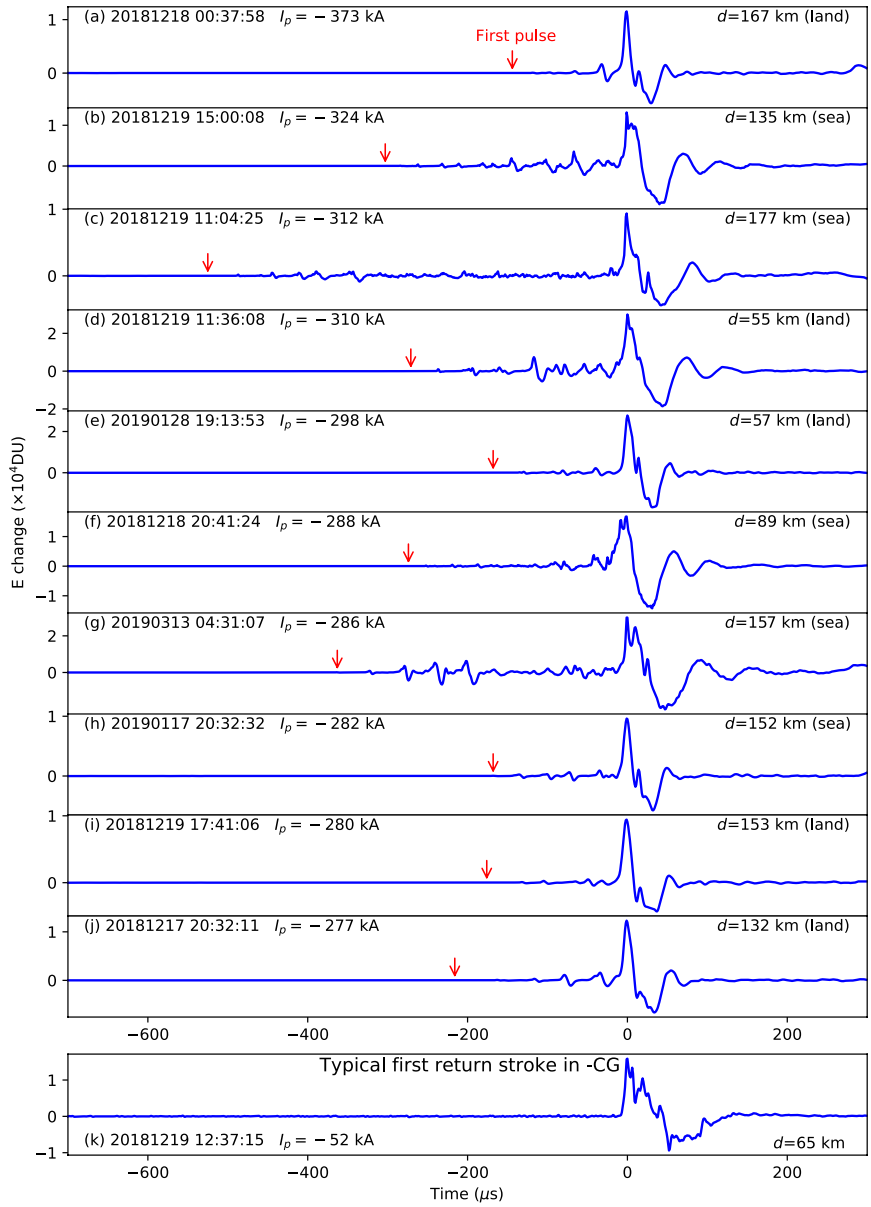

Figure 1. (a–j) E-change waveforms of the 10 strongest negative strokes. The red arrow indicates the first identified pulse before each stroke. The value of *d* represents the distance of the stroke to the site recording the plotted waveform. (k) Typical waveform of the first return stroke in a negative cloud-to-ground flash.

3. Results

3.1. E-Change Waveform

The most prominent feature of strong negative strokes in winter in Japan is that they produce E-change waveforms that are different from those produced by normal negative return strokes. Figures 1a–1j shows E-change waveforms of the 10 strongest negative strokes. As a direct comparison, Figure 1k shows the waveform of a typical first return stroke in a negative CG flash. The shape of stroke pulses in Figures 1a–1j are generally different from those of normal negative return strokes. Some common waveform characteristics of typical first return strokes in negative CG flashes, including much larger fall time than rising time, fine structure in the falling portion, and relatively small preceding leader pulses, cannot be seen in the strong strokes in Figures 1a–1j. More importantly, these strong strokes are preceded by discharges with very short

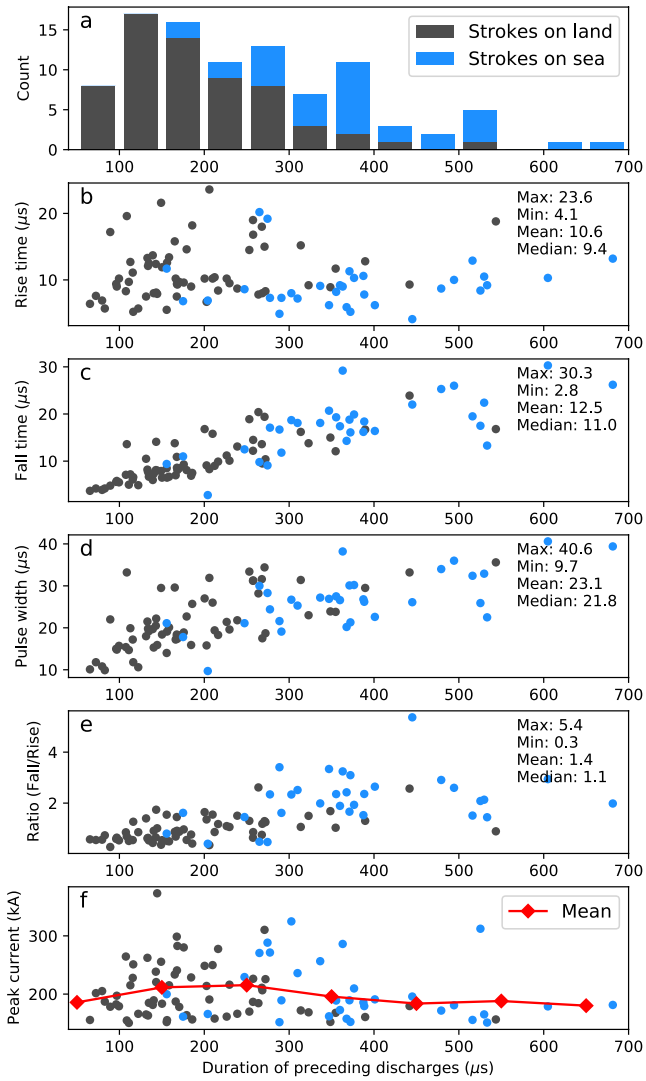

Figure 2. E-change waveform parameters of strong negative strokes and preceding discharges. (a) The distribution of durations of preceding discharges. Scatterplots of durations of preceding discharges versus (b) Rise time, (c) Fall time, (d) Pulse width, (e) The ratio of fall time to rise time, and (d) Peak currents of stroke pulses. Blue bars and points represent strokes on the sea and black ones on land. Red diamonds in panel (f) represent mean values of peak currents in each 100-μs range.

durations, generally shorter than 500 μs. Red arrows in Figures 1a–1j indicate the first identified pulses before these strokes. Details about the identification of the first pulses can be found in Wu et al. (2021).

In fact, almost all negative strokes with peak currents larger than 150 kA have similar features to those in Figures 1a–1j. Figure 2a shows the distribution of durations of preceding discharges (defined as the time difference between the first identified pulse in the flash and the peak of the stroke pulse). Three strokes with exceptionally long preceding discharges are not included here and will be described in more detail later. Excluding these three special cases, Figure 2a shows that all strokes with peak currents larger than 150 kA are preceded by discharges with durations shorter than 700 μs. The minimum and maximum durations in Figure 2a are 65.3 and 681.4 μs, respectively, with a mean value of 252.8 μs. Such short durations are due to fast downward negative leaders (velocity of one event is analyzed in Section 3.3) preceding the return stroke and the close proximity of winter thunderclouds to the ground. Furthermore, discharges preceding the first return stroke in normal negative CG flashes consist of PB and stepped leader processes. Pulses before these strong strokes may be somewhat similar to PB pulses but they cannot be divided into two clearly different stages corresponding to the PB and stepped leader processes. Enlarged waveforms of discharges preceding the strokes in Figures 1a–1j are shown in Figure S4 in Supporting Information S1.

Figures 2b–2e show statistics of pulse rise time, fall time, pulse width, and the ratio of fall time to rise time for these strokes. Definitions of these parameters are shown in Figure S5 in Supporting Information S1. Compared with parameters of E-change waveforms of first strokes in negative CG flashes reported in the literature (Rakov & Uman, 2003), it is clear that these strong strokes in winter have a larger rise time but smaller pulse width. As a result, the ratio of the fall time to rise time is relatively small, resulting in somewhat symmetric stroke pulses. However, it is important to note that the fall time, pulse width, and the ratio of fall time to rise time are dependent on the duration of preceding discharges as demonstrated in Figures 2c–2e. Similar results were also reported for special strokes in winter with durations of preceding discharges shorter than 1 ms (Wu et al., 2021). We can see that as the duration of preceding discharges increases, the fall time, the pulse width, and the ratio of fall time to rise time all increase, getting closer to waveform characteristics of first strokes in normal negative CG flashes. High correlations between duration of preceding discharges and waveform parameters of stroke pulses also indicate that both the stroke and preceding discharges are associated with the same channel, and a reasonable explanation is that preceding discharges are leader processes creating a channel in the virgin air and the stroke pulse is due to the return stroke traversing the same channel. Figure 2f shows that peak currents of strokes are also associated with durations of preceding discharges, which indicates that the strongest strokes usually have preceding discharges with durations of 200–300 μs, as can also be seen in Figures 1a–1j.

Three special cases have durations of preceding discharges of 188, 27, and 16 ms and peak currents of 187, 184, and 180 kA. Details of these three special cases are provided in Figures S6–S8 in Supporting Information S1. It is interesting to note that although durations of preceding discharges of these cases are orders of magnitudes larger than other cases, the stroke pulses are generally similar to those in Figures 1a–1j. Since these cases are uncommon and their peak currents are not exceptionally strong, we will not analyze these special cases in this study.

Waveforms of all 98 strokes with peak currents larger than 150 kA are provided in the data repository (see Acknowledgment). We can see that almost all waveforms are somewhat different from those of normal return strokes, although it is rather subjective to determine what kind of waveforms are "normal." The strongest stroke we found that looks very like a normal return stroke and was preceded by discharges with obvious two stages presumably corresponding to the PB and stepped leader has a peak current of −148 kA. Its E-change waveform is shown in Figure S9 in Supporting Information S1.

3.2. Current Reflection in Stroke Channels

An interesting feature of waveforms of these strong strokes is that a small pulse sometimes can be found superimposed on the negative cycle of the stroke pulse. Examples can be found in Figures 1a, 1c, 1h and 1i. Two strong pulses reported to be associated with downward TGFs in winter thunderstorms (Wada et al., 2020) also had such features. The origin of the small pulses is not yet clear. Here we demonstrate that the small pulses are due to the current reflection in return stroke channels.

First, it should be noted that features of the small pulse are varied; they are not always as pronounced as those reported by Wada et al. (2020) and are not always right at the negative cycle of the stroke pulse. Figures 3a–3d show some examples of small pulses with different features. The small pulses indicated by purple arrows are treated as the same phenomenon in the following analysis.

We found 62 strokes with recognizable small pulses such as those in Figures 3a–3d. These small pulses are identified as the most significant pulse between the main peak and the end of the negative cycle. Figures of their E-change waveforms are provided in the data repository. We calculated the time difference between the small pulse and the onset of the stroke pulse. The definition of the time difference, denoted as Δt, is illustrated in Figure 3a. The correlation between the time difference Δt and the duration of preceding discharges is shown in Figure 3e. We can see that the two parameters show a very strong correlation with a correlation coefficient of 0.81.

Our previous study demonstrated that when the duration of preceding discharges is very small, the preceding discharges are likely produced by a downward negative leader developing directly to the ground, and thus the duration is related to the stroke channel length (Wu et al., 2021). Therefore, the strong correlation in Figure 3e indicates that the time difference Δt is also related to the stroke channel length, and a reasonable explanation is that the small pulse is produced by the current reflection in the stroke channel.

Assuming that the reflected pulse is produced when the return stroke wave is reflected from the upper end of the channel, the slope of the linear regression line (which is 0.052) in Figure 3e equals the ratio of the leader velocity to the return stroke velocity. For the velocity of the downward negative leader, we have estimated that the velocity is about 3×10^6 m/s for cases with durations of preceding discharges smaller than 200 μs (Wu et al., 2021). The leader velocity of a strong stroke observed directly by the optical system LAPOS analyzed in Section 3.3 is about 5×10^6 m/s. If we use these values as the leader velocity, the return stroke velocity would be 5.8 to 9.6×10^7 m/s, which is slightly smaller than return stroke velocities reported in the literature (Rakov, 2007). However, considering the fact that the velocity decreases as the return stroke wave propagates and that most previous measurements mainly focused on velocities at the channel bottom, our result can be considered as a reasonable result. Moreover, the above estimation assumes a fixed upper end of the return stroke channel. In reality, the upper end may extend upward during the downward propagation of the negative leader, resulting in an underestimation of the return stroke velocity.

The above estimation demonstrates that the current reflection is a plausible explanation for the small pulses. It also provides supporting evidence that these special strokes are return strokes. The estimation is also consistent with the assumption of a downward negative leader with the velocity on the order of 10^6 m/s right before these strong strokes. It is also an expected result that strong negative return strokes are usually preceded by fast negative leaders (Nag & Cummins, 2017; Shi et al., 2019; Zhu et al., 2015).

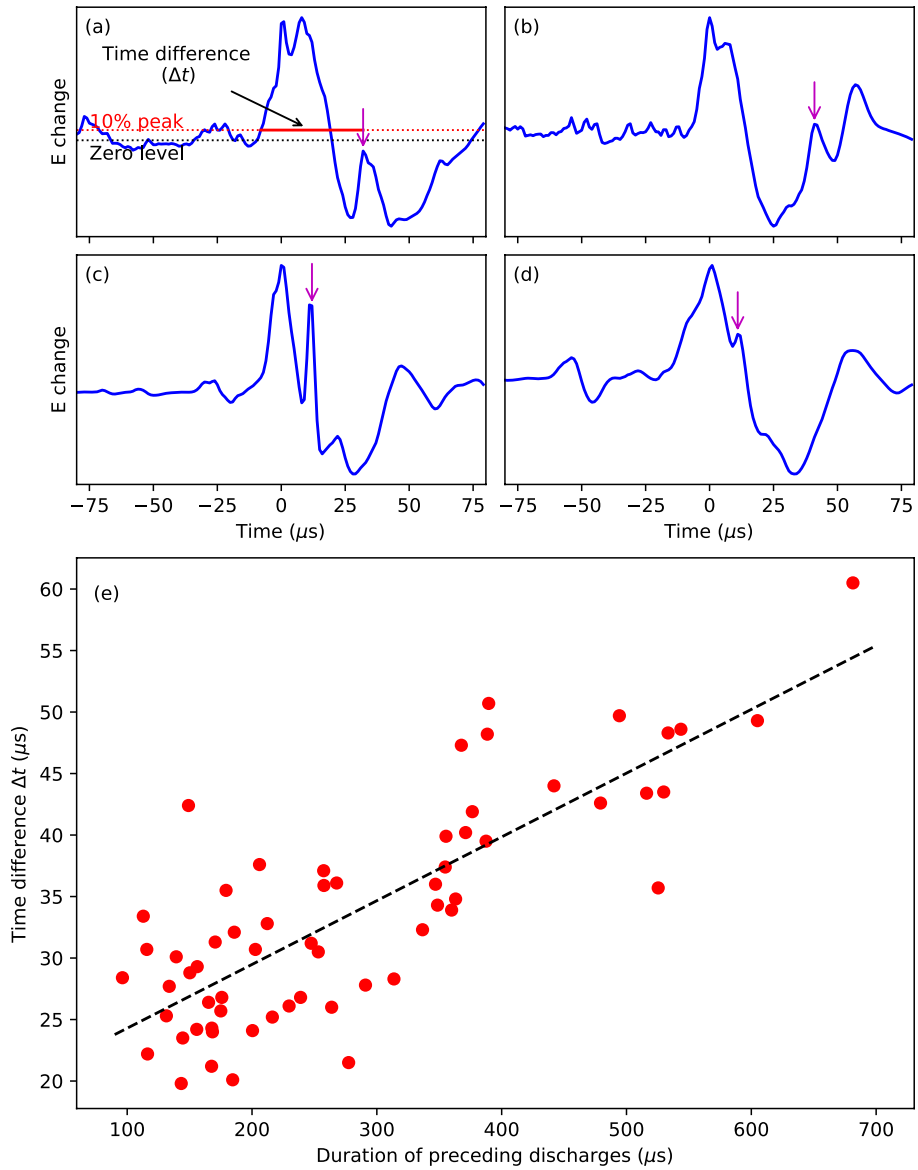

Figure 3. (a)–(d) Stroke pulses with different types of reflected pulses. Purple arrows indicate reflection pulses. The red horizontal line in panel (a) represents the definition of the time difference between the reflection pulse and the onset of the return stroke (Δt) (e) Correlation between the time difference Δt and the duration of preceding discharges.

3.3. A Strong Stroke Observed by the LAPOS

A negative stroke with a JLDN-reported peak current of −335 kA was observed by the high-speed optical system LAPOS, enabling us to directly estimate the speed of the return stroke and the preceding downward leader.

E-change waveforms recorded by two sites of the FALMA and light intensity waveforms recorded by the LAPOS are shown in Figure 4. Time zero corresponds to the first detected pulse indicated by the red arrow in Figure 4b. All FALMA sites were saturated by this stroke, and Figure 4a shows the least saturated waveform. We can see that the E-change waveform of this stroke is generally similar to those in Figures 1a–1j. Figure 4b shows the E-change waveform recorded by a site 6 km away. Due to the close distance, we can clearly identify the first pulse. The duration of preceding discharges is about 357 μs.

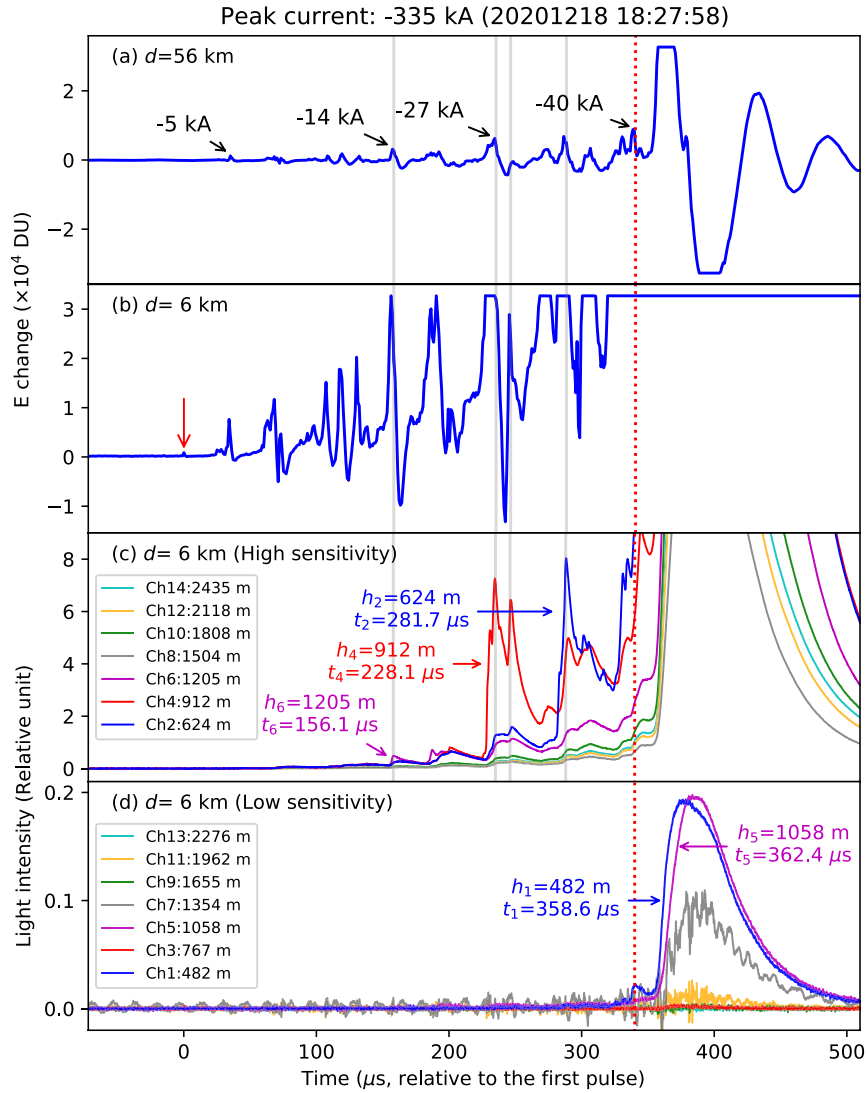

Figure 4. A stroke with a peak current of −335 kA observed by the lightning attachment process observation system (LAPOS) and the fast antenna lightning mapping array (FALMA). E-change waveforms observed by FALMA sites at distances of (a) 56 km and (b) 6 km. Waveforms of light intensity observed by (c) High-sensitivity photodiodes and (d) Low-sensitivity photodiodes of LAPOS. The red arrow in panel (b) indicates the first identified pulse before the stroke. Values of h and t represent the height and onset time of light pulses observed by the LAPOS.

Figure 4c shows the light intensity waveform recorded by the high-sensitivity photodiodes of the LAPOS. Similar waveforms from negative CG strokes were reported by Wang et al. (2015). We can see that the first clear light signal was detected by channel 6 at the height of 1,205 m and at the time of 156.1 μs. Note that the time corresponds to the onset of the pulse and is calculated as the time of 20% pulse peak (Huang et al., 2020). It is likely that before the time of 156.1 μs, the leader was propagating inside the thundercloud and thus could not be detected by the LAPOS. The second light pulse was detected by channel 4 at the height of 912 m at the time of 228.1 μs and the third by channel 2 at the height of 624 m and at the time of 281.7 μs. Variations of the height and time of these channels indicate a leader propagating downward, and no other light signals detected before these signals indicate that this flash started from inside the cloud. From channels 6 and 4, we can estimate that the speed of the downward leader is 4.1 $\times 10^6$ m/s, and from channels 4 and 2, the estimated speed is 5.4 $\times 10^6$ m/s. These values are one order of magnitude larger than the typical speed of stepped leaders before first return strokes in negative CG flashes but are similar to the speed of downward negative leaders preceding compact return strokes in winter thunderstorms (Wu et al., 2021).

Figure 4d shows the light intensity waveform recorded by the low-sensitivity photodiodes of the LAPOS. These light signals mainly correspond to the return stroke process. Two large pulses were detected by channels 1 and 5, from which we can estimate that the speed of the return stroke was 1.5×10^8 m/s, a typical return stroke speed. Channel 7 also detected a pulse but it was relatively weak and had large noise, probably because the return stroke wave already developed into the cloud. That channel 3 did not have any response may be due to a malfunction of the channel.

Assuming the light intensity recorded by the LAPOS is proportional to the peak current (Idone & Orville, 1985; Wang et al., 2005), we can roughly estimate the peak currents of the stepping processes of the downward negative leader. In Figures 4a and 4d, a leader pulse is observed by Channel 1 indicated by the red dashed line. The ratio of the light intensity of the leader pulse peak to the return stroke pulse peak measured by the same channel is 0.12. Neglecting current attenuation with height, we can estimate that the peak current of the leader pulse is about −40 kA. Peak currents of other leader pulses can be estimated from E-change magnitudes in Figure 4a by calculating the ratio to the E-change magnitude of the −40-kA leader pulse indicated by the red dashed line, assuming that the peak current of the leader pulse is proportional to the E-change magnitude of its radiation electric field. Peak currents of four pulses of leader steps are estimated as shown in Figure 4a. The peak currents range from −5 to −40 kA. These values are one to two orders of magnitude larger than peak currents of downward stepped leaders inferred from magnetic or electric field observations (Shen et al., 2019; Thomson et al., 1985; Williams & Brook, 1963) and upward negative leaders in triggered lightning or from tall objects (Miki et al., 2014; Pu et al., 2017; Watanabe et al., 2019; Zhou et al., 2012). In fact, strong strokes analyzed in this study are almost always preceded by clear leader pulses as shown in Figures 1a–1j, indicating strong peak currents of stepped leaders. A strong negative stroke reported by Lyu et al. (2015) was also preceded by large leader pulses. We speculate that strong negative strokes may be usually preceded by strong leader pulses.

The above analysis demonstrated unambiguously that the strong stroke in Figure 4 was preceded by a fast downward negative leader with large currents. The negative leader connected to the ground and initiated the return stroke, which produced the exceptionally strong pulse.

4. Discussion and Conclusion

In this study, we presented conclusive evidence that strong negative return strokes with peak currents larger than 150 kA in winter thunderstorms in Japan produce unusual E-change waveforms that are generally different from those produced by first return strokes in normal negative CG flashes. As lightning location systems such as NLDN in the US (e.g., Cummins & Murphy, 2009) and JLDN in Japan classify CG flashes based on waveform characteristics of return strokes, it is possible that some of these strongest negative return strokes in winter are not identified by these systems. In fact, the two strong strokes with peak currents of −260 kA and −197 kA reported to be associated with downward TGFs were identified as intracloud discharges by JLDN (Wada et al., 2020). The fact that few studies have investigated strong negative CG flashes or return strokes in winter may be simply due to the uncertainty in identifying strong negative strokes in winter.

The finding that the unusual pulses such as those in Figures 1a–1j are produced by return strokes makes it doubtful that whether they are directly associated with TGFs (Wada et al., 2020). It is well known that TGFs are usually associated with upward negative leaders in intracloud flashes (Cummer et al., 2015; Lu et al., 2010). Pu et al. (2020) also reported a downward TGF produced during a downward negative leader preceding a negative return stroke. We have demonstrated that these strong negative return strokes are preceded by a fast and powerful downward negative leader. Therefore, it is possible that it is actually the strong leader pulses right before negative return strokes, rather than the return strokes themselves, that are associated with TGFs.

The duration of the preceding leader pulses is closely related to the properties of the stroke pulse as demonstrated in Figure 2. Wu et al. (2021) recently reported that strokes with durations of preceding discharges shorter than 200 μs mostly occurred in mountain areas and were inferred to have very short (on average 300 m) channels and were named “compact strokes.” Wu et al. (2021) demonstrated that LBEs reported by Wu et al. (2014) were also compact strokes. Lyu et al. (2021) recently reported a type of strong pulses

that were located in the high mountains of the western US in summer. Those pulses share the same feature as pulses of strong strokes analyzed in this study: some small pulses with durations of a few hundred microseconds followed by a large pulse. Lyu et al. (2021) speculated that those pulses were produced by terrain-initiated upward positive leaders, which might be wrong if the pulses had the same nature as those analyzed in this study.

Finally, we point out that these strong negative strokes are likely "superbolts" observed by the WWLLN (Holzworth et al., 2019) and from the space (Ripoll et al., 2021). Holzworth et al. (2019) reported that most superbolts observed by the WWLLN occurred in winter, and the sea of Japan is one of the hotspots. Further, Holzworth et al. (2019) examined superbolts (with energy larger than 10^6 J) that were also observed by the ENTLN (Mallick et al., 2015), and they found that out of 18 matches, 14 were negative strokes with peak currents larger than 100 kA. Ripoll et al. (2021) reported that only 15% superbolts were positive CG flashes, compared with 28% of positive CG flashes during their observation. Ripoll et al. (2021) also found that compared with normal strokes, waveforms produced by superbolts have larger rise time and smaller fall time, "leading to a more symmetric ground wave." These characteristics are all consistent with the characteristics of strong negative strokes analyzed in this study. Lyu et al. (2021) also suggested that similar pulses detected in high mountains in the US may be related to superbolts.

Strong negative strokes reported in this study are largely unknown in the lightning research community. Now that we have demonstrated that they are undoubtedly returned strokes in negative CG flashes, more efforts should be made to clarify their physical mechanisms, conditions for their productions, and relationship with other lightning discharges and high-energy phenomena. It is also necessary to modify criteria employed by lightning location systems to classify return strokes.

Data Availability Statement

Related data can be found at https://doi.org/10.5281/zenodo.5150405.

Acknowledgments
This study was supported by the Ministry of Education, Culture, Sports, Science, and Technology of Japan (Grants 20H02129 and 21K03681).

References

Adachi, T. (2005). Characteristics of thunderstorm systems producing winter sprites in japan. *Journal of Geophysical Research*, *110*(D11). https://doi.org/10.1029/2004jd005012

Brook, M., Nakano, M., Krehbiel, P., & Takeuti, T. (1982). The electrical structure of the Hokuriku winter thunderstorms. *Journal of Geophysical Research*, *87*(C2), 1207. https://doi.org/10.1029/jc087ic02p01207

Cummer, S. A., Lyu, F., Briggs, M. S., Fitzpatrick, G., Roberts, O. J., & Dwyer, J. R. (2015). Lightning leader altitude progression in terrestrial gamma-ray flashes. *Geophysical Research Letters*, *42*(18), 7792–7798. https://doi.org/10.1002/2015gl065228

Cummins, K. L., & Murphy, M. J. (2009). An overview of lightning locating systems: History, techniques, and data uses, with an in-depth look at the US NLDN. *IEEE Transactions on Electromagnetic Compatibility*, *51*(3), 499–518. https://doi.org/10.1109/temc.2009.2023450

Hayakawa, M. (2004). Observation of sprites over the sea of Japan and conditions for lightning-induced sprites in winter. *Journal of Geophysical Research*, *109*(A1). https://doi.org/10.1029/2003ja009905

Holzworth, R. H., McCarthy, M. P., Brundell, J. B., Jacobson, A. R., & Rodger, C. J. (2019). Global distribution of superbolts. *Journal of Geophysical Research: Atmospheres*, *124*(17–18), 9996–10005. https://doi.org/10.1029/2019jd030975

Huang, H., Wang, D., Uman, M., Wu, T., & Takagi, N. (2020). Fine progression features of return stroke luminosity at the bottom of rocket-triggered lightning channels. *Journal of Atmospheric Electricity*, *39*(2), 57–69. https://doi.org/10.1541/jae.39.57

Idone, V. P., & Orville, R. E. (1985). Correlated peak relative light intensity and peak current in triggered lightning subsequent return strokes. *Journal of Geophysical Research*, *90*(D4), 6159. https://doi.org/10.1029/jd090id04p06159

Ishii, M., & Saito, M. (2009). Lightning electric field characteristics associated with transmission-line faults in winter. *IEEE Transactions on Electromagnetic Compatibility*, *51*(3), 459–465. https://doi.org/10.1109/temc.2009.2025496

Lu, G., Blakeslee, R. J., Li, J., Smith, D. M., Shao, X.-M., McCaul, E. W., et al. (2010). Lightning mapping observation of a terrestrial gamma-ray flash. *Geophysical Research Letters*, *37*(11). https://doi.org/10.1029/2010GL043494

Lyu, F., Cummer, S. A., Krehbiel, P. R., Rison, W., Bruning, E. C., & Rutledge, S. A. (2021). A distinct class of high peak-current lightning pulses over mountainous terrain in thunderstorms. *Geophysical Research Letters*, *48*(14). https://doi.org/10.1029/2021gl094153

Lyu, F., Cummer, S. A., & McTague, L. (2015). Insights into high peak current in-cloud lightning events during thunderstorms. *Geophysical Research Letters*, *42*(16), 6836–6843. https://doi.org/10.1002/2015GL065047

Mallick, S., Rakov, V., Hill, J., Ngin, T., Gamerota, W., Pilkey, J., et al. (2015). Performance characteristics of the ENTLN evaluated using rocket-triggered lightning data. *Electric Power Systems Research*, *118*, 15–28. https://doi.org/10.1016/j.epsr.2014.06.007

Matsudo, Y., Suzuki, T., Hayakawa, M., Yamashita, K., Ando, Y., Michimoto, K., & Korepanov, V. (2007). Characteristics of Japanese winter sprites and their parent lightning as estimated by VHF lightning and ELF transients. *Journal of Atmospheric and Solar-Terrestrial Physics*, *69*(12), 1431–1446. https://doi.org/10.1016/j.jastp.2007.05.002

Matsui, M., Michishita, K., & Yokoyama, S. (2019). Characteristics of negative flashes with multiple ground strike points located by the Japanese lightning detection network. *IEEE Transactions on Electromagnetic Compatibility*, *61*(3), 751–758. https://doi.org/10.1109/TEMC.2019.2913661

Miki, M., Miki, T., Asakawa, A., & Shindo, T. (2014). Characteristics of negative upward stepped leaders in positive upward lightning. Presented at the Xv International Conference on Atmospheric Electricity.
Nag, A., & Cummins, K. L. (2017). Negative first stroke leader characteristics in cloud-to-ground lightning over land and ocean. *Geophysical Research Letters*, *44*(4), 1973–1980. https://doi.org/10.1002/2016GL072270
Pu, Y., Cummer, S. A., Huang, A., Briggs, M., Mailyan, B., & Lesage, S. (2020). A satellite-detected terrestrial gamma ray flash produced by a cloud-to-ground lightning leader. *Geophysical Research Letters*, *47*(15). https://doi.org/10.1029/2020gl089427
Pu, Y., Jiang, R., Qie, X., Liu, M., Zhang, H., Fan, Y., & Wu, X. (2017). Upward negative leaders in positive triggered lightning: Stepping and branching in the initial stage. *Geophysical Research Letters*, *44*(13), 7029–7035. https://doi.org/10.1002/2017gl074228
Rakov, V. A. (2007). Lightning return stroke speed. *Journal of Lightning Research*, *1*, 80–89.
Rakov, V. A., & Uman, M. A. (2003). *Lightning: Physics and effects* (p. 154). Cambridge University Press.
Ripoll, J.-F., Farges, T., Malaspina, D. M., Cunningham, G. S., Lay, E. H., Hospodarsky, G. B., et al. (2021). Electromagnetic power of lightning superbolts from earth to space. *Nature Communications*, *12*(1). https://doi.org/10.1038/s41467-021-23740-6
Shen, Y., Chen, M., Du, Y., & Dong, W. (2019). Line charge densities and currents of downward negative leaders estimated from VHF images and VLF electric fields observed at close distances. *IEEE Transactions on Electromagnetic Compatibility*, *61*(5), 1507–1514. https://doi.org/10.1109/temc.2018.2864199
Shi, D., Wang, D., Wu, T., & Takagi, N. (2019). Correlation between the first return stroke of negative cg lightning and its preceding discharge processes. *Journal of Geophysical Research: Atmospheres*, *124*(15), 8501–8510. https://doi.org/10.1029/2019JD030593
Suzuki, T., Hayakawa, M., Matsudo, Y., & Michimoto, K. (2006). How do winter thundercloud systems generate sprite-inducing lightning in the Hokuriku area of Japan? *Geophysical Research Letters*, *33*(10). https://doi.org/10.1029/2005gl025433
Takeuti, T., Nakano, M., Brook, M., Raymond, D. J., & Krehbiel, P. (1978). The anomalous winter thunderstorms of the Hokuriku coast. *Journal of Geophysical Research*, *83*(C5), 2385. https://doi.org/10.1029/jc083ic05p02385
Thomson, E. M., Uman, M. A., & Beasley, W. H. (1985). Speed and current for lightning stepped leaders near ground as determined from electric field records. *Journal of Geophysical Research*, *90*(D5), 8136–8142. https://doi.org/10.1029/jd090id05p08136
Wada, Y., Enoto, T., Nakamura, Y., Morimoto, T., Sato, M., Ushio, T., et al. (2020). High peak-current lightning discharges associated with downward terrestrial gamma-ray flashes. *Journal of Geophysical Research: Atmospheres*, *125*(4), e2019JD031730. https://doi.org/10.1029/2019JD031730
Wang, D., Takagi, N., Gamerota, W. R., Uman, M. A., Hill, J. D., & Jordan, D. M. (2013). Initiation processes of return strokes in rocket-triggered lightning. *Journal of Geophysical Research: Atmospheres*, *118*(17), 9880–9888. https://doi.org/10.1002/jgrd.50766
Wang, D., Takagi, N., Gamerota, W. R., Uman, M. A., & Jordan, D. M. (2015). Lightning attachment processes of three natural lightning discharges. *Journal of Geophysical Research: Atmospheres*, *120*(20). https://doi.org/10.1002/2015jd023734
Wang, D., Takagi, N., Watanabe, T., Rakov, V., Uman, M., Rambo, K., & Stapleton, M. (2005). A comparison of channel-base currents and optical signals for rocket-triggered lightning strokes. *Atmospheric Research*, *76*(1–4), 412–422. https://doi.org/10.1016/j.atmosres.2004.11.025
Wang, D., Zheng, D., Wu, T., & Takagi, N. (2021). Winter positive cloud-to-ground lightning flashes observed by LMA in Japan. *IEEJ Transactions on Electrical and Electronic Engineering*, *16*(3), 402–411. https://doi.org/10.1002/tee.23310
Watanabe, N., Nag, A., Diendorfer, G., Pichler, H., Schulz, W., Rakov, V. A., & Rassoul, H. K. (2019). Characteristics of currents in upward lightning flashes initiated from the Gaisberg tower. *IEEE Transactions on Electromagnetic Compatibility*, *61*(3), 705–718. https://doi.org/10.1109/temc.2019.2916047
Williams, D. P., & Brook, M. (1963). Magnetic measurements of thunderstorm currents: 1. Continuing currents in lightning. *Journal of Geophysical Research*, *68*(10), 3243–3247. https://doi.org/10.1029/jz068i010p03243
Wu, T., Wang, D., & Takagi, N. (2018). Lightning mapping with an array of fast antennas. *Geophysical Research Letters*, *45*(8), 3698–3705. https://doi.org/10.1002/2018GL077628
Wu, T., Wang, D., & Takagi, N. (2020a). Multiple-stroke positive cloud-to-ground lightning observed by the falma in winter thunderstorms in japan. *Journal of Geophysical Research: Atmospheres*, *125*(20), e2020JD033039. https://doi.org/10.1029/2020JD033039
Wu, T., Wang, D., & Takagi, N. (2020b). Upward negative leaders in positive upward lightning in winter: Propagation velocities, electric field change waveforms, and triggering mechanism. *Journal of Geophysical Research: Atmospheres*, *125*(16), e2020JD032851. https://doi.org/10.1029/2020JD032851
Wu, T., Wang, D., & Takagi, N. (2021). Compact lightning strokes in winter thunderstorms. *Journal of Geophysical Research: Atmospheres*, *n/a*(n/a), e2021JD034932. https://doi.org/10.1029/2021JD034932
Wu, T., Yoshida, S., Ushio, T., Kawasaki, Z., Takayanagi, Y., & Wang, D. (2014). Large bipolar lightning discharge events in winter thunderstorms in Japan. *Journal of Geophysical Research: Atmospheres*, *119*(2), 555–566. https://doi.org/10.1002/2013JD020369
Zhou, H., Diendorfer, G., Thottappillil, R., Pichler, H., & Mair, M. (2012). Characteristics of upward positive lightning flashes initiated from the Gaisberg tower. *Journal of Geophysical Research: Atmospheres*, *117*(D6). https://doi.org/10.1029/2011JD016903
Zhu, Y., Rakov, V. A., Mallick, S., & Tran, M. D. (2015). Characterization of negative cloud-to-ground lightning in Florida. *Journal of Atmospheric and Solar-Terrestrial Physics*, *136*, 8–15. https://doi.org/10.1016/j.jastp.2015.08.006